High Isolation Quad-Element SWB-MIMO Antenna with Dual Band-Notch for ISM and WLAN Band Wireless Applications

Gaurav Saxena[1], Utkarsh Gupta[1], Shashikant Shukla[1], Utkarsh Shukla[1], Shipra Bharti[1], Y K Awasthi[2], Chintakindi Sanjay[3], Wigdan Aref Mohammed Saif[3], Himanshu Singh[4]

[1]Microwave and Optical Communication Laboratory, Department of Electronics & Communication Engineering, Galgotia College of Engineering and Technology, Greater Noida, UP India-201306
[2]Electronics & Communication Engineering, Manav Rachna International Institute of Research and Studies, Faridabad, HR India-121004
[3]Industrial Engineering Department, College of Engineering, King Saud University, P.O. Box. 800, Riyadh 11451, Saudi Arabia
[4]Department of Physics, Hindu College, University of Delhi, New Delhi, 110017, India
Corresponding author: Y K Awasthi (e-mail: yash_ips79@rediffmail.com), gaurav.saxena@galgotiacollege.edu

ABSTRACT A quad-element super-wideband (2-20GHz) MIMO antenna including dual notched-band response at WiMAX (3.30-3.70GHz) and satellite-band (6.99-8.09GHz) is designed on RO3035 with total dimension of 118mm×86mm×1.67mm. Unique decoupling structure has been deployed to enhance the isolation (>20dB) between two antenna elements. The fundamental properties of MIMO antennas like bandwidth ratio (10:1), isolation (>18dB), gain (4.14dB), Envelop Correlation-Coefficient (<0.0065), Total Active Reflection-Coefficient (< 0dB), Channel Capacity Loss (<0.25bps/Hz) and radiation patterns are also investigated in order to determine their practicality. Measurement and simulation results of the proposed SWB-MIMO antenna from 2 to 20GHz indicate that it will be the suitable candidate for wireless and biomedical applications.

INDEX TERMS Multiple-Input-Multiple-Output (MIMO), Super-Wideband (SWB), Defected Ground Structure (DGS), Metasurface (MS).

I. INTRODUCTION

SUPER-wideband antenna technology is increasingly being used in wireless communication applications to cover both short and long range transmission. Significant benefits given by SWB technology, particularly in terms of larger channel capacity and enhanced timing precision, have made the technology more appealing and necessary for a wide range of possible wireless communication. Higher bit-rate over the wideband is achieved by designing SWB MIMO antennas. Moreover, in today's era, many individuals die as a result of cancer illnesses, and in the majority of cases, the main cause of death is a late and ineffective diagnosis. Ahmed B.T. et al [1], proposed super wideband MIMO antenna with triple-band notch characteristics for avoiding the interference between near field devices. Elhabchi, M [2] suggest a novel U-shaped SWB MIMO antenna by using monopole antenna technique to reduce the loading Q of the antenna and enhance the bandwidth. Chaudhari, A.D. et.al. [3] designed and developed quasi-Yagi type MIMO antenna for high precision sensing application for accurate diagnosis of these cancer tissues. Super wideband MIMO antenna [4-8] with dual and triple-band notched characteristics has been discussed by using CSRR/SRR and band stop filter structure imposed on patch and ground. Ramanujam, P et.al.[9] suggest miniaturized monopole based SWB MIMO antenna to cover the 0.7-18.5GHz bandwidth to cover L-Ku microwave band. Kumar, P et.al. [10] designed and discussed about SWB MIMO antenna for IoT application with improved isolation by using decoupling structure on the ground which prevent current from energized antenna to 50Ω terminated antenna. Ullah, H., Rahman et.al. [11] and Singhal, S [12] proposed a new model of wide band and super wideband MIMO antenna with improved diversity performance with respect of ECC, DG, TARC and CCL for practical wireless 4G LTE advanced and high channel capacity wireless applications. In [13]-[20] to mitigate band interference, an antenna with multiple band-notch capability must be designed with bandstop filters. The need for a MIMO antenna comes from the fact that multiple antennas may enhance the data-rate of an operational band by N-folds, where N is the number of antennas on the corresponding MIMO antenna. Using diverse decoupling structures to enhance the isolation between elements and also improves the diversity performance in the real environment. Awan, W.A et.al. [21] suggest SWB antenna with notched characteristics by using genetic algorithm which is useful to improve the antenna parameters. In [22-23] Hussain, M. et.al. designed frequency reconfigurable dual-band CPW based wideband and conformal antenna for Wi-Max and WLAN application having militarized size. This antenna also used in

portable devices like mobile phone, tablet and laptops. Khurshid, A et.al.[24] designed and discuss MIMO antenna having exotic diversity performance with high isolation for enhancing channel capacity and data speed. In this article, a dual notched single element SWB antenna is designed initially, then by the design of novel decoupling structure with common ground to turn the antenna into a MIMO. Section-2 of this article is presenting the design procedure of the proposed antenna. Section-3 have all simulated and measured results related to the antennas. Section-4 concludes the findings of the design.

II. ANTENNA DESIGN AND RESULT ANALYSIS

Rogers RO3035 with a dielectric constant of 3.6, loss tangent of 0.0015, and thickness of 1.6mm is used to make the proposed SWB antenna.

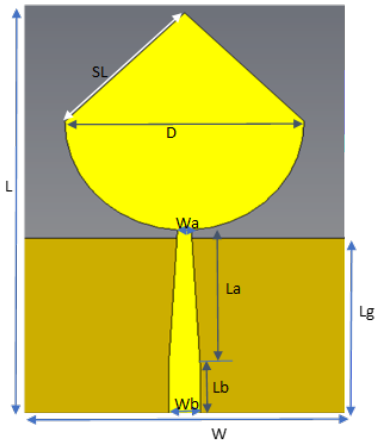

FIGURE 1. Geometry of the designed single element SWB antenna.

As far as antenna design is concerned, the dimensions of radiating element including feed line are generally calculated at minimum operational frequency and the radiating element can take many different forms, including circular, semi-circular, rectangular, heptagonal, hexagonal, and fractal shapes. Input impedance of these radiating elements is usually higher than 100 ohms. Thus, to match the 50 ohms impedance in wide-bandwidth, a taper microstrip line is required between the radiating device and the antenna connector.

The geometry of the single element antenna without any filter is shown in Figure 1, with working frequency range of 2-20 GHz. The radiating element has semi-circular shape embedded with a triangle on top of it. To match the input impedance of the radiating element, a trapezoidal taper 50 ohms feeding line with a length of 6mm is employed. Copper laminates with a thickness of 0.035 mm is used to make the radiation patch and the ground plane. All the simulated s-parameter results are hereby shown in the current section for proposed design using CST studio suite. The antenna is designed with a defected ground structure (DGS) to enhance the bandwidth as well.

TABLE I. Dimensions of single element SWB antenna with dual notch

Parameter	Value (mm)	Parameter	Value(mm)
L	49.00	L1	9.06
Lg	21.00	L2	10.80
La	16.00	L3	6.90
Lb	6.00	L4	1.80
SL	18.38	W1	0.30
D	26.00	W2	0.80
W	35.00		
Wa	1.50		
Wb	3.40		

All of the dimensional parameters of the proposed design are listed in Table I. The proposed structure has a tiny area of $49\times35mm^2$, which is significantly less than competing structures with similar bands and geometries. For the proposed band of 2-20GHz, simulation results for the single element SWB antenna are considerably below -10dB as shown in Figure 2.

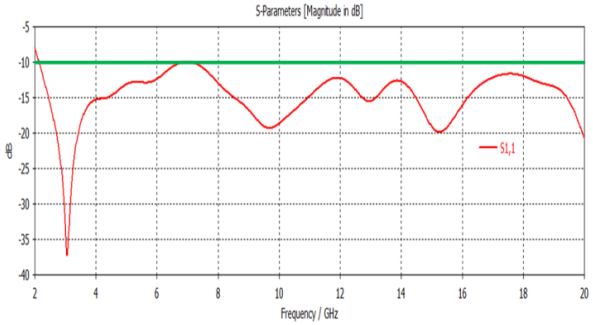

FIGURE 2. Simulated results of single element SWB antenna.

This SWB bandwidth makes the antenna susceptible to interference from other widely deployed systems near to it. Thus, the next step is to introduce notch filters that work at two frequency bands, namely, 3.5 GHz for WiMAX and 7.5 GHz for X-band downlink satellite. The 3.5 GHz filter is a half-wavelength U-shaped slot within the radiating patch. Finally, the 7.5 GHz filter is a half-wavelength U-shaped slot within the feeding line to mitigate the interference as illustrated in Figure 3. U-shaped slots length of filter 1 and 2 is calculated by equation (1)

$$L = \frac{c}{2\times f\times\sqrt{\varepsilon r}} \quad (1)$$

where, f = frequency c = speed of light L = Length of notch ε_r = Dielectric constant

Figure 3 shows the simulated and prototype geometry of dual band-notched SWB antenna and Figure 4 depicts the corresponding simulated & measured S_{11} parameter of the antenna. The first filter operates in the 3.19–3.81 GHz range, whereas the second filter operates in the 6.99–8.07 GHz band, according to the results.

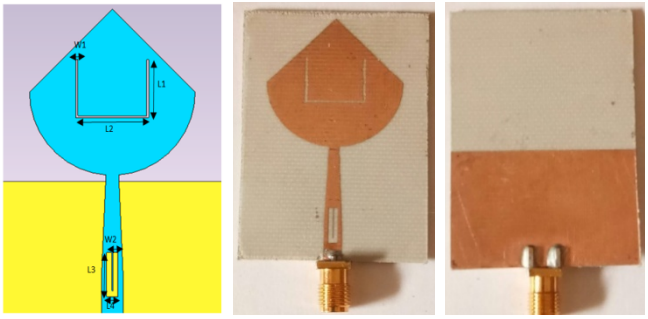

FIGURE 3. Simulated geometry and prototype of dual band-notched SWB single element antenna.

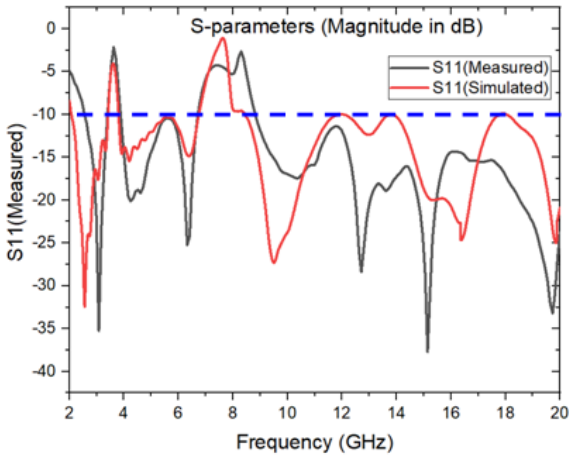

FIGURE 4. Simulated and measured s-parameters for dual band-notched SWB antenna.

In today's world, significant channel capacity and SWB bandwidth to handle the large data are necessary, which a single element cannot provide. As a result, the suggested antenna is turned into a quad-elements MIMO antenna using an appropriate isolation technique which is very essential to enhance the diversity performance of MIMO. The proposed MIMO antenna is fabricated on Rogers RO3035 (lossy) substrate and measured by using Agilent Technologies N5247A vector network analyser to validate the simulation results. Photograph of a fabricated single element antenna shown in Figure 14. Figure 16 (a) and (b) is the photograph of a fabricated four element SWB MIMO antenna.

III. MIMO ANTENNA DESIGN AND DISCUSSION OF RESULTS

To construct SWB two-element MIMO antenna, a pair of the previously designed dual band-notched SWB antenna is used. The spacing between the two elements of the MIMO antenna is chosen in such a way to have isolation between them higher than 15dB [16]. A diamond-shaped geometrical conducting barrier between the gaps of radiating elements to promote isolation, and a decoupling structure at ground is also designed for additional isolation, as shown in Figure 5. Table II shows the physical dimensions of the final band-notched two-element SWB-MIMO antenna. Simulated S_{12} and S_{22} results of the band-notched two-element SWB-MIMO antenna are presented in Figure 6. From the results, the return loss is less than -10dB except the band-notched at 3.19–3.81 GHz, and 6.99–8.08 GHz.

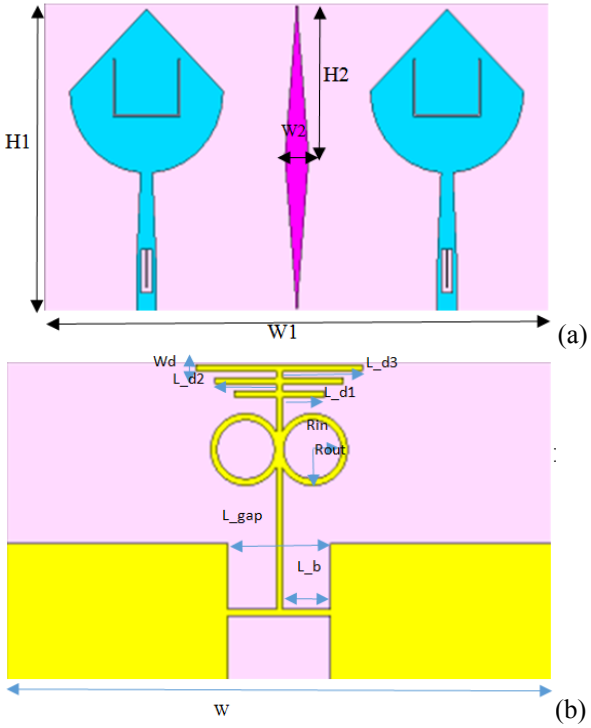

FIGURE 5. Geometrical view of two-element SWB MIMO antenna with (a) a diamond-shaped geometrical conducting barrier (b) a decoupling structure at ground.

TABLE II. Dimensions of decoupling structure available at top and ground of Figure 5

Parameter	Value(mm)	Parameter	Value(mm)
L-gap	16.00	H1	49.00
L_b	7.50	H2	24.50
Rin	4.50	W1	86.00
Rout	5.50	W2	4.00
L_d1	7.00		
L_d2	10.00		
L_d3	13.00		
W_d	1.00		

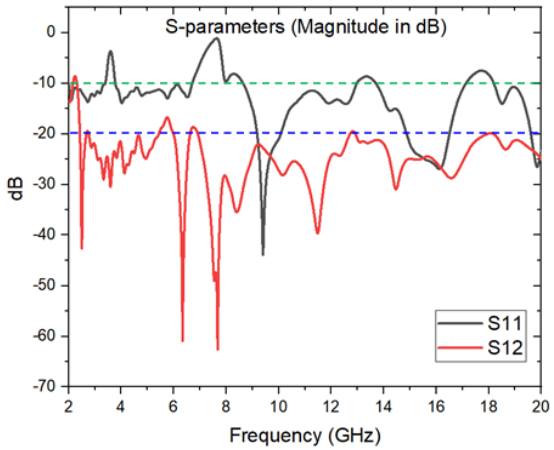

FIGURE 6. Simulated S_{11} and S_{12} results of the two-element SWB-MIMO antenna.

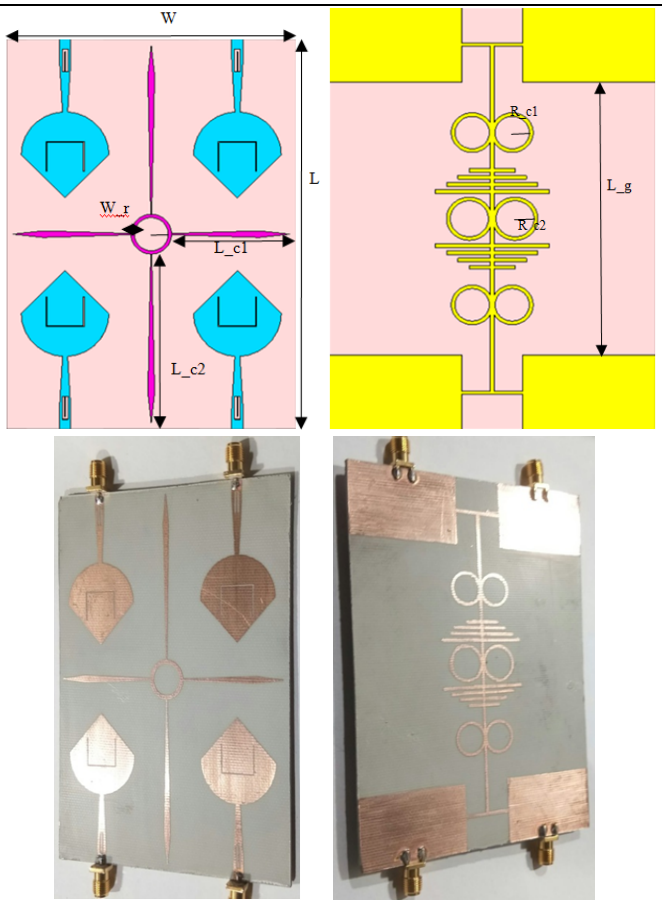

(a) (b)

FIGURE 7. The proposed quad-element SWB-MIMO antenna simulated and prototype (a) Front view (b) Back view.

Isolation is also noticed more than 20dB for intended band of frequency from 2–20 GHz. Moreover, to add more similar elements in the aforementioned design to further enhance the channel capacity of the MIMO system. A quad-element MIMO antenna is designed with almost similar results as shown in Figure 7.

TABLE III. Dimensions of proposed four-element SWB MIMO antenna

Parameter	Value(mm)	Parameter	Value (mm)
L	118.00	L_g	76.00
L_c1	37.00	R_c1	4.00
L_c2	53.00	R_c2	5.00
R_c	5.00		
W	86.00		
W_r	1.00		

Figure 7 shows the quad-element SWB-MIMO antenna with up-down parallel feed configuration. To improve isolation between quad-element a four sword-shaped structure attached with a circular ring between the elements and a common ground is designed as shown in Figure 7 (b). Table III gives the geometrical dimensions of the final quad-element SWB-MIMO antenna.

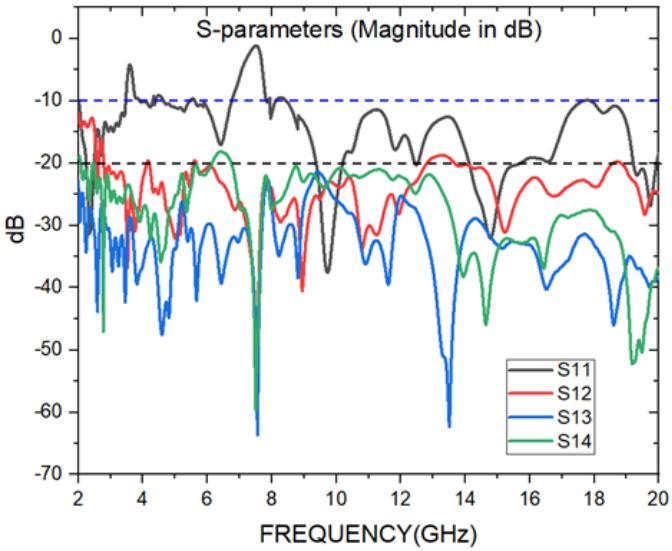

FIGURE 8. Simulated results (S_{11}, S_{12}, S_{13}, and S_{14}) of quad-element SWB-MIMO antenna.

SWB-MIMO antenna (a) S_{11}, (b) S_{12}, (c) S_{13}, and (d) S_{14}. Figure 8 and Figure 9 show the measured & simulated s-parameter results of the designed MIMO antenna. It can be noticed that, the refection parameter S_{11} is lower than -10dB except the notched-bands for intended bandwidth, and isolation (S_{12}, S_{13}, and S_{14}) between the elements is higher than 20dB. Figure 10 shows the gain of the proposed design which is in the range of 4.53 to 6.96dB in the intended bandwidth and Figure 11 shows the omini-directional type radiation patterns.

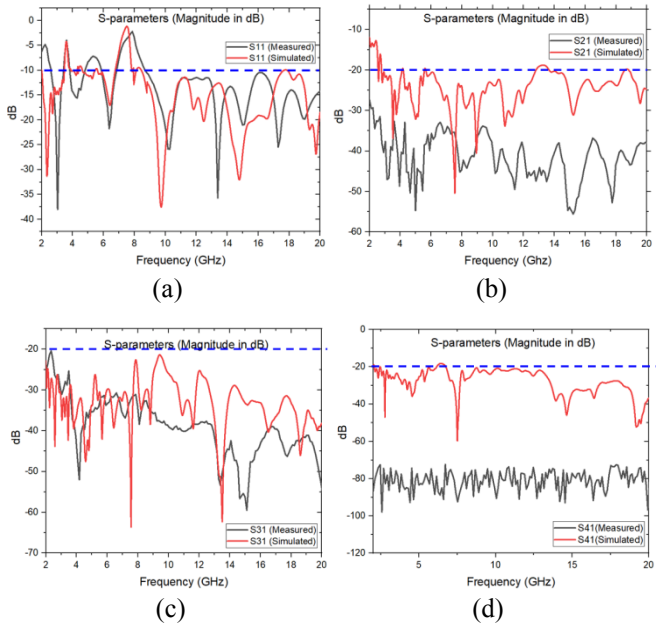

FIGURE 9. Measured and simulated results of the quad-element.

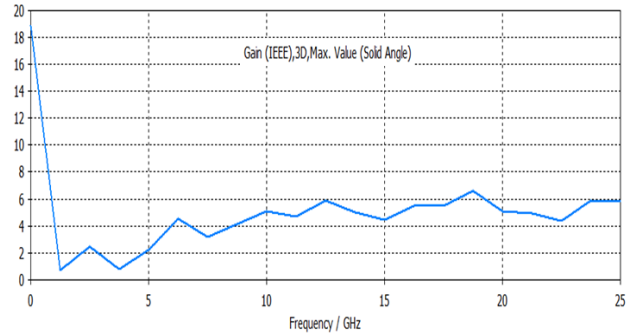

FIGURE 10. Simulated antenna gain of the proposed design.

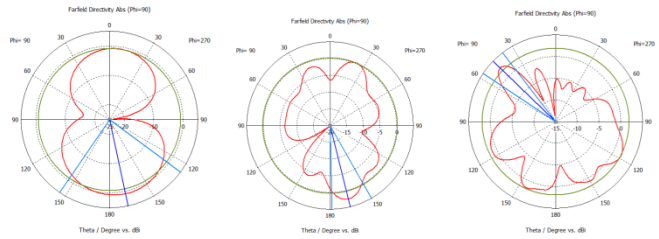

FIGURE 11. Simulated far-field radiation patterns at (a) 2.0GHz (b) 11GHz (c) 20GHz.

SPECIFIC ABSORPTION RATE

The penetration of electric field intensity in the human brain tissue near-field environment yields the SAR value of that electronic equipment [14]-[15] as shown in Figure 12. SAR is frequently averaged over a small sample volume (typically 1g to 10g of tissue) or the full body. SAR estimation of the head is done for 2.4 and 5.5 GHz frequency. The values of radius of skin, bone, and brain are 79.324, 75, and 65 mm, respectively, for this SAR estimate. The estimated value of SAR is less than 1.6 W/kg for the proposed antenna as shown in Table IV, for all parameters listed in Table V. This SAR performance is investigated without any plastic jacket or cover [14]-[15]-[27].

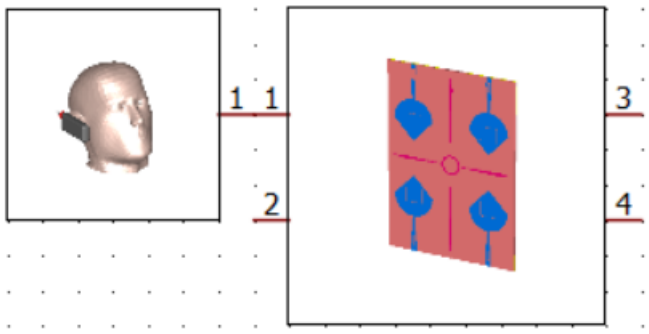

FIGURE 12. Simulated SAR setup of the SWB-MIMO antenna.

TABLE IV. Parameters of the human head used for calculation of specific absorption rate by the proposed antenna at constant permeability

Type	Bio-tissue skin	Bio-tissue bone	Bio-tissue Brain
Density(ρ), kg/m^3	1100	1850	1030
Thermal Conductivity(σ)	0.293	0.41	1.13
Heat capacity, kJ/K/kg	3.5	1.3	3.675
Blood flow, W/K/m^3	9100	3400	40,000
Metabolism rate, W/m^3	1620	610	7100

TABLE V. SAR values near the human head at the different resonant frequencies when the distance between the human head and MIMO antenna is 15mm

Specific Absorption Rate, W/kg			
2.4GHz		5.5GHz	
1(g)	10(g)	1(g)	10(g)
0.048	0.026	0.053	0.032

where (r) is the model's thermal conductivity in S/m, Erms (r) is the rms electric field in V/m, ρ(r) is the sample density in kg/m3, and V is the sample volume in m^3. SAR is a function of input power, with a calculating power of 100 mW.

IV. DIVERSITY PERFORMANCE OF QUAD-ELEMENT MIMO

In wireless communications systems, diversity techniques are employed to increase performance across fading-channels. Multiple copies of the same information signal are delivered through two or more communication channels to the recipient in such a system. There are various results presented here in this section in which ECC, diversity gain, channel capacity, etc. The Envelope Correlation coefficient is an essential antenna parameter for MIMO antennas since it indicates the independency of distinct antenna elements' radiation patterns [14]-[15].

The Envelope Correlation Coefficient for the proposed antenna is less than 0.007 shown in Figure 13, which is substantially below the desired threshold value (0.5), implying that the elements of the presented design are well separated and have independent radiation patterns.

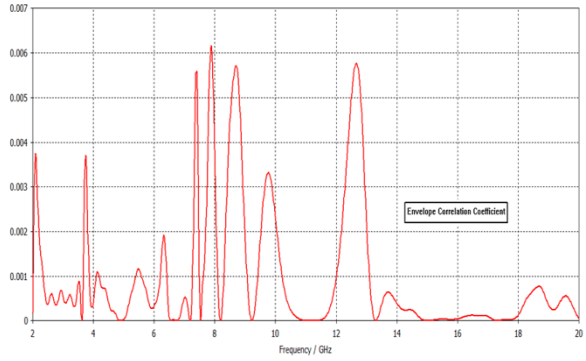

FIGURE 13. Simulated ECC of the designed SWB-MIMO antenna.

ECC from S-parameter is calculated by equation (2) [14]-[15], [25]-[26].

$$ECC(\rho_{ij}) = \frac{\left|S^*_{ii}S_{ij} + S^*_{ji}S_{jj}\right|^2}{\left(1-\left|S_{ii}\right|^2-\left|S_{ji}\right|^2\right)\left(1-\left|S_{jj}\right|^2-\left|S_{ij}\right|^2\right)} \quad (2)$$

Where S_{ii} and S_{ij} denotes return loss and insertion loss of i^{th} antenna when j^{th} antenna terminated with 50Ω load and i^{th} antenna is energized.

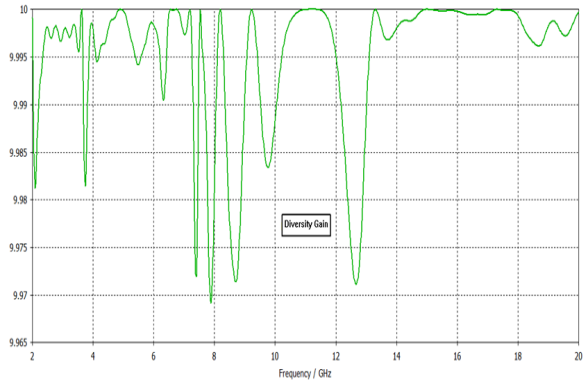

FIGURE 14. Simulated diversity gain for the proposed SWB-MIMO antenna.

Directive Gain (DG) has been calculated with equation (3) [14]-[15] in terms of ECC. It provides how much SNR benefits of MIMO antenna with respect to SISO antenna. For uncorrelated ECC = 0 system its ideal value 10dB and practical value >9.5dB.

$$DG = 10\sqrt{1-(ECC)^2} \quad (3)$$

Total active reflection coefficient (TARC) is the ratio of total reflected power in the MIMO system at all ports to the total power incident and it is calculated by equation (4) [14]-[15].

$$TARC = \frac{\sum_{n=1}^{N}\left|b_i\right|^2}{\sum_{n=1}^{N}\left|a_i\right|^2} \quad (4)$$

Where b_i and a_i denotes the reflected and incident power. Furthermore, to reduce necessary receive SNR (Signal-to-noise ratio) for a given bit-error-rate (BER), averaged across the fading is known as diversity gain. This is reduction in fading margin that is gained by the antennas to reduce fading.

In general, greater DG values are thought to signify better MIMO antenna performance. In Figure 14, it is seen that the diversity gain for the antenna is higher than 9.96 dB, this will undoubtedly explain the given antenna's higher signal to interference ratio. Hence, the proposed antenna's diversity gain also allows it to operate at low transmission power without signal loss, making it a very efficient antenna [25-26].

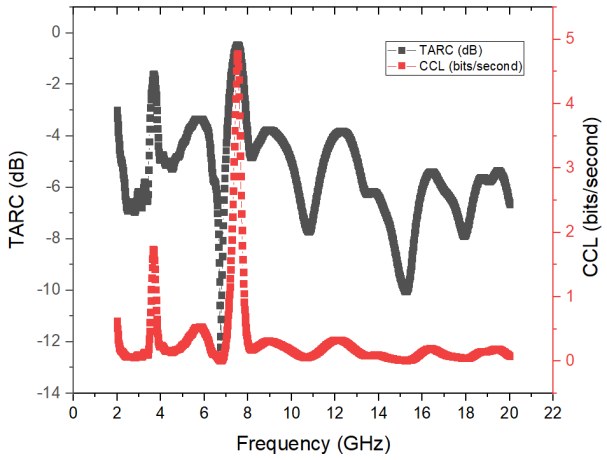

FIGURE 15. Simulated CCL and TARC of the proposed antenna.

As demonstrated in Figure 13, the proposed design's TARC and CCL have permissible values. TARC denotes the entire MIMO antenna elements' return loss.

TABLE VI. Comparison table of proposed MIMO antenna with existing literature

Size (λ_o^2)	Bandwidth (GHz)	Gain (dBi)	Isolation (dB)	ECC	Designing Approach/ Notched Bands
1.8[3]	1.37-16	5.5	16	<0.01	Quasi Yagi Type/2
2.91[5]	1.21-34	3.5	15	0.25	CPW Line/2
1.45[8]	1.3-40	5.5	15	0.01	CPW Line/3
1.4[14]	1.5-40	7.5	20	0.005	Monopole with step impedance feeding/1
12.84 [16]	0.97-35	5.2	19.8	0.005	Modified elliptical self-complimentary based/3
0.6 [Proposed]	**2-20**	**6.2**	**20**	**0.006**	**Monopole with decoupling/2**

V. CONCLUSION

A quad-element SWB-MIMO antenna with two band-notches has been built, with better agreement between simulated and measured results over the desired bandwidth of 2–20GHz. All of the parameters of MIMO antennas have been justified in order to establish their usefulness, including bandwidth ratio, isolation, directive gain, envelope correlation-coefficient, total active reflection-coefficient, channel capacity loss, and radiation patterns. In TABLE VI, the proposed MIMO antenna compared with existing literature and found suitable for wireless application with exotic diversity performance. This design has been deemed as a good choice for wireless and biological applications based on the above results and information.

REFERENCES

[1] Ahmed, B.T., Carreras, D.C. and Marin, E.G., 2021. Design and Implementation of Super Wide Band Triple Band-Notched MIMO Antennas. Wireless Personal Communications, pp.1-22.

[2] Elhabchi, M., Srifi, M.N. and Touahni, R., 2020. A novel modified U-shaped microstrip antenna for super wide band (SWB) applications. Analog Integrated Circuits and Signal Processing, 102(3), pp.571-578.

[3] Chaudhari, A.D. and Ray, K.P., 2021. A single-layer compact four-element quasi-Yagi MIMO antenna design for super-wideband response. AEU-International Journal of Electronics and Communications, 138, p.153878.

[4] Yu, C., Yang, S., Chen, Y., Wang, W., Zhang, L., Li, B. and Wang, L., 2020. A SuperWideband and high isolation MIMO antenna system using a windmill-shaped decoupling structure. IEEE Access, 8, pp.115767-115777.

[5] Bhattacharya, A., Roy, B. and Bhattacharjee, A.K., 2021. Compact, Isolation Enhanced, Band-Notched SWB–MIMO Antenna Suited for Wireless Personal Communications. Wireless Personal Communications, 116(3), pp.1575-1592.

[6] Raheja, D.K., Kumar, S. and Kanaujia, B.K., 2020. Compact quasi-elliptical-self complementary four-port super-wideband MIMO antenna with dual band elimination characteristics. AEU-International Journal of Electronics and Communications, 114, p.153001.

[7] Palanisamy, P. and Subramani, M., 2020. Design and experimental analysis of miniaturized octa-port UWB/SWB-MIMO antenna with triple-band rejection characteristics. IETE Journal of Research, pp.1-15.

[8] Kumar, P., Urooj, S. and Alrowais, F., 2020. Design of quad-port MIMO/Diversity antenna with triple-band elimination characteristics for super-wideband applications. Sensors, 20(3), p.624.

[9] Ramanujam, P., Venkatesan, P.R., Arumugam, C. and Ponnusamy, M., 2020. Design of miniaturized super wideband printed monopole antenna operating from 0.7 to 18.5 GHz. AEU-International Journal of Electronics and Communications, 123, p.153273.

[10] Kumar, P., Urooj, S. and Malibari, A., 2020. Design and Implementation of Quad Element Super-Wideband MIMO Antenna for IoT Applications. IEEE Access, 8, pp.226697-226704.

[11] Ullah, H., Rahman, S.U., Cao, Q., Khan, I. and Ullah, H., 2020. Design of SWB MIMO antenna with extremely wideband isolation. Electronics, 9(1), p.194.

[12] Singhal, S., 2021. Feather-shaped super wideband MIMO antenna. International Journal of Microwave and Wireless Technologies, 13(1), pp.94-102.

[13] Das, S., Mitra, D. and Chaudhuri, S.R.B., 2021. Fractal loaded planar Super Wide Band four element MIMO antennas for THz applications. Nano Communication Networks, 30, p.100374.

[14] Saxena, G., Jain, P. and Awasthi, Y.K., 2020. High diversity gain super-wideband single band-notch MIMO antenna for multiple wireless applications. IET Microwaves, Antennas & Propagation, 14(1), pp.109-119.

[15] Saxena, G., Awasthi, Y.K. and Jain, P., 2020. High Isolation and High Gain SuperWideband (0.33-10 THz) MIMO Antenna for THz Applications. Optik, 223, p.165335.

[16] Raheja, D.K., Kanaujia, B.K. and Kumar, S., 2019. Low profile four-port super-wideband multiple-input-multiple-output antenna with triple band rejection characteristics. International Journal of RF and Microwave Computer-Aided Engineering, 29(10), p.21831.

[17] Irshad Khan, M., Khattak, M.I., Rahman, S.U., Qazi, A.B., Telba, A.A. and Sebak, A., 2020. Design and investigation of modern UWB-MIMO antenna with optimized isolation. Micromachines, 11(4), p.432.

[18] Garg, R.K., Singhal, S. and Tomar, R., 2021. A CPW Fed Clown-Shaped Super Wideband Antenna. Progress In Electromagnetics Research Letters, 99, pp.159-167.

[19] Bahmanzadeh, F. and Mohajeri, F., SWB MIMO Antenna with Dual Band Rejection Characteristics and Polarization Diversity for UWB Applications. Iranian Journal of Science and Technology, Transactions of Electrical Engineering, 2021. https://doi.org/10.1007/s40998-022-00575-5

[20] Raheja, D.K., Kumar, S., Kanaujia, B.K., Palaniswamy, S.K., Thipparaju, R.R. and Kanagasabai, M., 2021. Truncated elliptical Self-Complementary antenna with QuadBand notches for SWB MIMO systems. AEU-International Journal of Electronics and Communications, 131, p.153608.

[21] Awan, W.A., Zaidi, A., Hussain, M., Hussain, N. and Syed, I., 2021. The design of a wideband antenna with notching characteristics for small devices using a genetic algorithm. Mathematics, 9(17), p.2113.

[22] Hussain, M. and Nadeem, N., 2019, July. A co-planer waveguide feed dual band antenna with frequency reconfigurability for WLAN and WiMax systems. In 2019 International Conference on Electrical, Communication, and Computer Engineering (ICECCE) (pp. 1-5). IEEE.

[23] Hussain, M., Ali, E.M., Awan, W.A., Hussain, N., Alibakhshikenari, M., Virdee, B.S. and Falcone, F., 2022. Electronically reconfigurable and conformal triband antenna for wireless communications systems and portable devices. Plos one, 17(12), p.e0276922.

[24] Khurshid, A., Dong, J., Ahmad, M.S. and Shi, R., 2022. Optimized super-wideband MIMO antenna with high isolation for IoT applications. *Micromachines*, *13*(4), p.514.

[25] Kumar, A., Saxena, G., Kumar, P., Awasthi, Y.K., Jain, P., Singhwal, S.S. and Ranjan, P., 2022. Quad-band circularly polarized super-wideband MIMO antenna for wireless applications. *International Journal of RF and Microwave Computer-Aided Engineering*, *32*(6), p.e23129.

[26] Lodhi, D., Bhaskar, S. and Singhal, S., 2023. Quad port wheel shaped superwideband MIMO antenna. *Journal of Ambient Intelligence and Humanized Computing*, pp.1-17.

[27] Hussain, M., Awan, W.A., Alzaidi, M.S., Hussain, N., Ali, E.M. and Falcone, F., 2023. Metamaterials and Their Application in the Performance Enhancement of Reconfigurable Antennas: A Review. *Micromachines*, *14*(2), p.349.